Heliyon 6 (2020) e04958

Contents lists available at ScienceDirect

Heliyon

journal homepage: www.cell.com/heliyon

Research article

Synthesis, molecular docking, antiplasmodial and antioxidant activities of new sulfonamido-pepetide derivatives

Efeturi A. Onoabedje [a,c,*], Akachukwu Ibezim [b,**], Uchechukwu C. Okoro [a], Sanjay Batra [c]

[a] Department of Pure & Industrial Chemistry, Faculty of Physical Sciences, University of Nigeria, Nsukka, Enugu State, Nigeria
[b] Department of Pharmaceutical and Medicinal Chemistry, Faculty of Pharmaceutical Sciences, University of Nigeria, Nsukka, Enugu State, Nigeria
[c] Division of Medicinal & Process Chemistry, Central Drug Research Institute, Lucknow, UP, India

ARTICLE INFO

Keywords:
Organic chemistry
Pharmaceutical chemistry
Synthesis
Dipeptides
Sulphonamides
Antimalarial
Antioxidant
N-myristoyltransferase
Docking

ABSTRACT

Twenty-three new series of toluene-sulfonamide dipeptide derivatives were synthesized and screened for antiplasmodial and antioxidant potencies. Many of the derivatives were active against *Plasmodium falciparum* with IC_{50} ranging from 3.20 – 9.10 μM. The ability of compounds **7h**, **7m** and **7n** (IC_{50} of 7.53, 7.21 and 6.01 μg/mL respectively) to scavenge DPPH free radicals were comparable to that of ascorbic acid. Additionally, molecular docking disclosed that four compounds exhibited theoretical inhibition constant at submicromolar concentrations (K_i = 0.72, 0.75, 0.57, and 0.53 μM respectively) compare to the reference ligand (a pyrazole sulfonamide; K_i = 0.01 μM). Overall, some of the derivatives possess antimalarial property as well as the ability to inhibit oxidative stress in malaria pathophysiology; and hence, are good candidates for further antimalarial drug research.

1. Introduction

Sulfonamides are group of sulfa drugs which illicit their antimalarial action by disruption of folate biosynthesis pathway which is critical to parasitic survival. Sulfanilamide, sulfadiazine and dapsone were amongst the first sulfa drugs to be employed in the treatment of malaria infections [1, 2].

Malaria is one of the most widespread and fatal parasitic disease in humans, basically caused by *Plasmodium falciparum* and *Plasmodium vivax*, but the deadliest, is *P. falciparum* [3, 4]. The disease was responsible for 405,000 deaths out of which 228 million cases were recorded in 2018 alone [5]. In spite of the extensive control measures to combat the disease and the continued efforts of Medicines for Malaria Venture (MMV) to support new discovery of several chemotypes which are undergoing various stages of clinical development; the emerging resistance to currently used drugs, including the artemisinin-based combination therapies, has motivated new interest to discover/design new antimalaria agents especially ones with new mode of actions [6, 7, 8].

Several natural and synthetic peptides have shown various degrees of inhibitory activities against *P. falciparum* growth [9, 10]. Linear short peptides such as di, tri, tetra, and penta peptides; and their cyclic analogues with micromolar range of antimalarial activity have been reported [11, 12]. Moreover, short peptides incorporating sulfonamide groups have been reported to possess numerous biological properties such as antimicrobial and antimalarial activities [13, 14, 15]. For example, molecules **V**, **VI** and **VII** hybrids of peptides and sulfonyl groups possess antimalarial plasmodium-selective proteasome inhibitory property at nanomolar ranges [16]. In addition, the introduction of sulfonamide group into peptides usually provides improved proteolytic stability, hydrogen-bonding possibilities and improved biological activities [17].

Malaria physiopathogenesis is associated with increase in the amount of oxygen free radicals and reduction in the number of antioxidant enzymes [18, 19]. While in the host RBCs, *P. falciparum* digests haemoglobin leading to the production of heme. This heme subsequently activates the generation of reactive oxygen species resulting in anamia and apoptesis due to oxidative stress [20, 21, 22]. The stress leads to molecular and cellular damage which is implicated in many disease conditions like cancer, bacterial infections and aging. Therefore, drug candidates with antiplasmodial potency that can scavenge oxygen free radicals are highly sought after in antimalarial development [23, 24].

P. falciparum undergoes series of changes inside the infected red blood cells (RBCs), beginning from ring stage to trophozoites, then continues to schizonts and finally to merozoites which egress and invade another

* Corresponding author.
** Corresponding author.
E-mail addresses: efeturi.onoabedje@unn.edu.ng (E.A. Onoabedje), akachukwu.ibezim@unn.edu.ng (A. Ibezim).

https://doi.org/10.1016/j.heliyon.2020.e04958
Received 6 July 2020; Received in revised form 14 August 2020; Accepted 14 September 2020
2405-8440/© 2020 Published by Elsevier Ltd. This is an open access article under the CC BY-NC-ND license (http://creativecommons.org/licenses/by-nc-nd/4.0/).

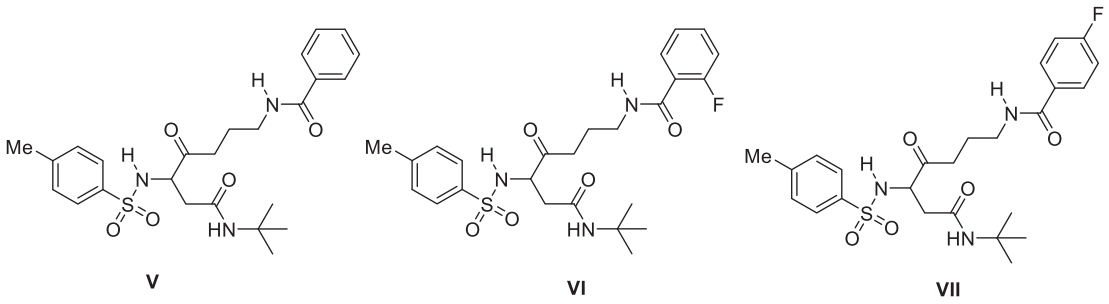

RBCs. Therefore, enzymes which are involved in the pathogen's life stage progression or viability are regarded as attractive drug targets for antimalarial development. One of such enzymes is N-myristoyltransferase (NMT), the catalyst for the co- and post-translational transfer of myristoyl group from the cofactor to N-terminal glycine protein substrate, which is necessary for the activities of inner membrane complex (IMC). The invasion of RBCs by merozoites is propelled by molecular motor complex which has been assembled by inner IMC. So inhibition of NMT paralyses IMC activities and subsequently *P. falciparum* viability [25, 26, 27].

In continuation of our search for antimalarial compounds in the sulfonamide-carboxamide hybrid family; the synthesis, *in-vitro* antiplasmodial and antioxidant activities of twenty-three new sulfonamide-dipeptide derivatives were described. Furthermore, selected relevant molecular descriptors, used to evaluate basic pharmacokinetic features of compounds, were computed computationally. Finally, we employed molecular docking to assess binding affinity of the derivatives for *P. falciparum* NMT (PfNMT) homology model because of the importance of the enzyme as relatively new validated antimalarial drug target.

2. Material and methods

2.1. General information

Unless otherwise stated all reactions were performed in non-dry glassware under an air atmosphere and were monitored by analytical thin layer chromatography (TLC). TLC was performed on pre-coated silica gel plates. After elution, plate was visualized under UV illumination at 254 nm for UV active materials. The melting points were recorded on a hot stage apparatus and are uncorrected. IR spectra were recorded using a FTIR spectrophotometer. ^{1}H NMR and ^{13}C NMR spectra were recorded on 400 MHz NMR spectrometers with DMSO-d^6 as solvent, using TMS as an internal standard (chemical shifts in ppm). Peak multiplicities of ^{1}H-NMR signals were designated as s (singlet), brs (broad singlet), d (doublet), dd (doublet of doublet), t (triplet), q (quartet), p (pentet) m (multiplet) etc. Coupling constants (J) are in Hz. The ESI-MS were recorded on triple quadrupole Mass spectrometer. Column chromatography was performed using silica gel (100–200 mesh). Analytical grade solvents for the column chromatography were used as received.

2.2. General procedures for the synthesis of dipeptide-sulfonamides

To 2-(4-Methylphenylsulfonamido)propanoic acid (1.0 equiv.), EDC.HCl (1.2 equiv) and HOBT (1.2 equiv) was added DCM (5.0 mL) and DIPEA (2.0 equiv.) and the reaction mixture stirred for 20 min at room temperature. Thereafter, 2-amino-*N*-substitutedphenylpropanamide (1.0 equiv.) was added and the entire reaction was allowed to stir at room temperature overnight. The reaction mixture was diluted with DCM (20mL), and subsequently washed with 5% bicarbonate (3 × 20 mL), 1.0 M HCl (3 × 30 mL), and brine (3 × 30 mL). The organic layer was dried over Na_2SO_4, filtered and evaporated under vacuum to provide the crude product, which was purified by column chromatography (10–70% EA/Hexane) to afford the desire product.

2-(4-methylphenylsulfonamido)-*N*-(1-oxo-1-(phenylamino) propan-2-yl)propanamide (7a). Yield: 60%; a white solid, mp 198–200 °C; R_f = 0.40 (Hexane: EtOAc, 3:7, v/v). IR ($CHCl_3$) ν_{max}: 1308, 1439(S=O), 1638, 1685 (C=O), 3196, 3278, 3337(N–H) cm^{-1}.^{1}H NMR (400 MHz, DMSO-d_6): δ = 1.07 (d, J = 7.1 Hz, 3H), 1.2 (d, J = 7.0 Hz, 3H), 2.36 (s, 3H),3.87-3.80 (m, 1H), 4.24 (p, J = 7.2 Hz, 1H), 7.05 (t, J = 7.4 Hz, 1H), 7.36-7.28 (m, 4H), 7.69-7.57 (m, 4H), 7.92 (d, J = 8.4 Hz, 1H), 8.09 (d, J = 7.3 Hz, 1H), 9.91 (s, 1H). ^{13}C NMR (100 MHz, DMSO-d_6): 18.7, 19.4, 21.4, 49.2, 52.1, 119.6, 123.8, 127.1, 129.2, 129.9, 138.6, 139.3, 143.0, 171.3, 171.5 (C=O). MS (ESI+): m/z = 390.3. ESI-HR-MS calculated for $C_{19}H_{23}N_3O_4S$ (M^++H): 390.1488, found: 390.1483.

2-(4-methylphenylsulfonamido)-*N*-(1-oxo-1-(*p*-tolylamino) propan-2-yl)propanamide (7b). Yield: 54%; a white solid, mp 218–220 °C; R_f = 0.40 (Hexane: EtOAc, 3:7, v/v). IR ($CHCl_3$) ν_{max}: 1329, 1402 (S=O), 1634 (C=O), 3242, 3741(N–H) cm^{-1}.^{1}H NMR (400 MHz, DMSO-d_6): δ = 1.06 (d, J = 7.0 Hz, 3H), 1.19 (d, J = 7.0 Hz, 3H), 2.25 (s, 3H),2.36 (s, 3H), 3.79–3.86 (m, 1H), 4.22 (p, J = 7.2 Hz, 1H), 7.11 (d, J = 8.3 Hz, 2H), 7.5 (d, J = 8.1 Hz, 2H), 7.46 (d, J = 8.4 Hz, 2H), 7.68 (d, J = 8.2 Hz, 2H), 7.92 (d, J = 8.3 Hz, 1H), 8.07 (d, J = 7.4 Hz, 1H), 9.82 (s, 1H). ^{13}C NMR (100 MHz, DMSO-d_6): 18.7, 19.4, 20.9, 21.4, 49.2, 52.1, 119.7, 127.1, 129.6, 129.9, 132.8 136.8, 138.5, 143.1, 171.0, 171.4 (C=O). MS (ESI+): m/z = 404.4. ESI-HR-MS calculated for $C_{21}H_{27}N_3O_4S$ (M^++H): 404.1644, found: 404.1640.

***N*-(4-methoxyphenyl)-2-(2-(4-methylphenylsulfonamido)prop-anamido)propanamide (7c)**. Yield: 68%; a white solid, mp 223–225 °C; R_f = 0.51 (Hexane: EtOAc, 1:9, v/v). IR ($CHCl_3$) ν_{max}: 1339, 1446 (S=O), 1634, 1880 (C=O), 3253, 3307 (N–H) cm^{-1}.^{1}H NMR (400 MHz, DMSO-d_6): δ = 1.06 (d, J = 7.1 Hz, 3H), 1.19 (d, J = 7.0 Hz, 3H), 2.36 (s, 3H), 3.72 (s, 3H),3.77–3.90 (m,1H), 4.21(p, J = 7.1 Hz, 1H), 6.88 (d, J = 9.0 Hz, 2H), 7.35 (d, J = 8.1 Hz, 2H), 7.49 (d, J = 9.1 Hz, 2H), 7.68 (d, J = 8.3 Hz, 2H), 7.92 (s, br, 1H), 8.06 (d, J = 7.4 Hz, 1H), 9.77 (s, 1H). ^{13}C NMR (100 MHz, DMSO-d_6): 18.7, 19.4, 21.4, 31.2, 49.1, 52.1, 55.6, 114.3, 121.1, 127.1, 129.9, 132.4, 138.5, 143.0, 155.7, 170.7, 171.4 (C=O). MS (ESI+): m/z = 420.3. ESI-HR-MS calculated for $C_{20}H_{25}N_3O_5S$ (M^++H): 420.1593, found: 420.1589.

***N*-(4-isopropylphenyl)-2-(2-(4-methylphenylsulfonamido)prop-anamido)propanamide (7d)**. Yield: 51%; a white solid, mp 213–215 °C; R_f = 0.45 (Hexane: EtOAc, 3:7, v/v). IR ($CHCl_3$) ν_{max}: 1318, 1415 (S=O), 1633, 1684 (C=O), 3259, 3338 (N–H) cm^{-1}.^{1}H NMR (400 MHz, DMSO-d_6): δ = 1.11 (d, J = 7.1 Hz, 3H), 1.23 (t, J = 7.1 Hz, 9H), 2.04 (s, 3H), 2.88 (q, J = 6.9 Hz,1H), 3.84–3.91 (m, 1H), 4.28(p, J = 7.2 Hz, 1H), 7.22 (d, J = 8.6 Hz, 2H), 7.40 (d, J = 8.1 Hz, 2H), 7.53 (d, J = 8.5 Hz, 2H), 7.72 (d, J = 8.3 Hz, 2H), 7.97 (d, J = 8.4 Hz, 1H), 8.12 (d, J = 7.4 Hz, 1H), 9.88 (s, 1H). ^{13}C NMR (100 MHz, DMSO-d_6): 18.7, 19.4, 21.4, 24.4, 33.3, 49.2, 52.1, 119.7, 126.9, 127.1, 129.9, 137.1, 138.6, 143.0, 143.9, 171.0, 171.4 (C=O). MS (ESI+): m/z = 432.4. ESI-HR-MS calculated for $C_{22}H_{29}N_3O_4S$ (M^++H): 432.1957, found: 432.1951.

***N*-(4-bromophenyl)-2-(2-(4-methylphenylsulfonamido)prop-anamido)propanamide (7e)**. Yield: 52%; a white solid, mp 250–252 °C; R_f = 0.67 (Hexane: EtOAc, 3:7, v/v). IR ($CHCl_3$) ν_{max}: 1311, 1396, 1450 (S=O), 1643, 1688 (C=O), 3181, 3275, 3343 (N–H) cm^{-1}.^{1}H NMR (400

MHz, DMSO-d_6): $\delta = 1.06$ (d, $J = 7.0$ Hz, 3H), 1.20 (d, $J = 7.1$ Hz, 3H), 2.36 (s, 3H), 3.84(p, $J = 7.3$ Hz,1H), 4.21(p, $J = 7.1$ Hz, 1H), 7.35 (d, $J = 8.1$ Hz, 2H), 7.49 (d, $J = 8.9$ Hz, 2H), 7.56 (d, $J = 8.9$ Hz, 2H), 7.67 (d, $J = 8.2$ Hz, 2H), 7.91 (d, $J = 8.4$ Hz, 1H), 8.12 (d, $J = 7.3$ Hz, 1H), 10.06 (s, 1H). ^{13}C NMR (100 MHz, DMSO-d_6): 18.5, 19.4, 21.4, 49.3, 52.0, 115.4, 121.6, 127.1, 129.9, 132.0, 138.6, 138.7, 143.0, 171.5, 171.5 (C=O). MS (ESI+): m/z = 468.2. ESI-HR-MS calculated for $C_{19}H_{22}$ BrN_3O_4S (M^++H): 468.0593, found: 468.0588.

***N*-(4-chlorophenyl)-2-(2-(4-methylphenylsulfonamido)propanamido)propanamide (7f)**. Yield: 58%; a white solid, mp 238–240 °C; $R_f = 0.74$ (Hexane: EtOAc, 3:7, v/v). IR ($CHCl_3$) ν_{max}: 1336, 1399, 1438 (S=O), 1607, 1692 (C=O), 3199, 3284, 3344 (N–H) cm^{-1}.^{1}H NMR (400 MHz, DMSO-d_6): $\delta = 1.06$ (d, $J = 7.1$ Hz, 3H), 1.20 (d, $J = 7.1$ Hz, 3H), 2.36 (s, 3H), 3.84(p, $J = 7.0$ Hz,1H), 4.21(p, $J = 7.1$ Hz, 1H), 7.34–7.37 (m, 4H), 7.59–7.62 (m,2H), 7.67 (d, $J = 8.2$ Hz, 2H), 7.91 (d, $J = 7.6$ Hz, `1H), 8.12 (d, J = 7.24 Hz, 1H), 10.06 (s, 1H). ^{13}C NMR (100 MHz, DMSO-d_6): 18.5, 19.4, 21.4, 49.3, 52.0, 121.2, 127.1, 127.4, 129.1, 129.9, 138.3, 138.6, 143.0, 171.4, 171.5 (C=O). MS (ESI+): m/z = 446.2. ESI-HR-MS calculated for $C_{19}H_{22}ClN_3O_4S$ (M^++H): 424.1098, found: 424.1095.

***N*-(4-fluorophenyl)-2-(2-(4-methylphenylsulfonamido)propanamido)propanamide (7g)**. Yield: 71%; a white solid, mp 215–217 °C; $R_f = 0.59$ (Hexane: EtOAc, 3:7, v/v).IR ($CHCl_3$) ν_{max}: 1340, 1381, 1411 (S=O), 1638, 1692 (C=O), 3201, 3286, 3348 (N–H) cm^{-1}.^{1}H NMR (400 MHz, DMSO-d_6): $\delta = 1.06$ (d, $J = 7.0$ Hz, 3H), 1.20 (d, $J = 7.1$ Hz, 3H), 2.36 (s, 3H), 3.83(p, $J = 7.5$ Hz, 1H), 4.21 (p, $J = 7.1$ Hz, 1H), 7.92 (d, $J = 8.2$ Hz, 1H), 8.10 (d, $J = 7.3$ Hz, 1H), 9.98 (s, 1H). ^{13}C NMR (100 MHz, DMSO-d_6): 18.6, 19.4, 21.4, 49.2, 52.1, 115.7, 115.9, 121.4, 121.4, 127.1, 129.9, 135.7, 138.5, 143.1, 157.6, 159.5, 171.2, 171.5 (C=O). ESI-HR-MS calculated for $C_{19}H_{22}$ FN_3O_4S (M^++H): 408.1393, found: 408.1392.

***N*-(3-chlorophenyl)-2-(2-(4-methylphenylsulfonamido)propanamido)propanamide(7h)**. Yield: 58%; a white solid, mp 168–170 °C; $R_f = 0.78$ (Hexane: EtOAc, 3:7, v/v).IR ($CHCl_3$) ν_{max}: 1240, 1323, 1423 (S=O), 1661 (C=O), 3336 (N–H) cm^{-1}.^{1}H NMR (400 MHz, DMSO-d_6): $\delta = 0.99$ (d, $J = 7.0$ Hz, 3H), 1.13 (d, $J = 7.1$ Hz, 3H), 2.29 (s, 3H), 3.77(p, $J = 7.2$ Hz, 1H), 4.13(p, $J = 7.1$ Hz, 1H), 7.03–7.06 (m, 1H), 7.24–7.29 (m, 3H), 7.35–7.38 (m,1H), 7.60 (d, $J = 8.3$ Hz, 2H), 7.72 (t, $J = 2.0$ Hz, 1H), 7.84 (d, $J = 8.4$ Hz, 1H),8.06 (d, $J = 7.1$ Hz, 1H), 10.04 (s, 1H). ^{13}C NMR (100 MHz, DMSO-d_6): 18.4, 19.4, 21.4, 49.3, 52.0, 118.0, 119.1, 123.6, 127.1, 129.9, 131.0, 133.6, 138.6, 140.8, 143.0, 171.5, 171.7 (C=O). MS (ESI + Na): m/z = 446.2. ESI-HR-MS calculated for $C_{19}H_{22}$ ClN_3O_4S (M^++H): 424.1098, found: 424.1094.

***N*-(3-fluorophenyl)-2-(2-(4-methylphenylsulfonamido)propanamido)propanamide (7i)**. Yield: 55%; a white solid, mp 192–194 °C; $R_f = 0.64$ (Hexane: EtOAc, 3:7, v/v).IR ($CHCl_3$) ν_{max}: 1321, 1381, 1441 (S=O), 1642, 1688 (C=O), 3196, 3277, 3347 (N–H) cm^{-1}.^{1}H NMR (400 MHz, DMSO-d_6): $\delta = 1.06$ (d, $J = 7.0$ Hz, 3H), 1.20 (d, $J = 7.1$ Hz, 3H), 2.36 (s, 3H), 3.84(p, $J = 7.1$ Hz, 1H), 4.21 (p, $J = 7.1$ Hz, 1H), 6.86–6.91 (m,1H), 7.28–7.32 (m, 1H), 7.33–7.36 (m, 3H),7.55–7.59 (m, 1H), 7.68 (d, J = 8.3 Hz, 2H),7.92 (d, $J = 7.7$ Hz, 1H), 8.13 (d, $J = 7.2$ Hz, 1H), 10.14 (s, 1H). ^{13}C NMR (100 MHz, DMSO-d_6): 18.4, 19.4, 21.4, 49.3, 52.0, 106.3, 106.5, 110.2, 110.4, 115.4, 127.1, 129.9, 130.8, 130.9, 138.6, 141.0, 141.1, 143.0, 157.6, 161.6, 163.6, 171.5, 171.7 (C=O).). MS (ESI + Na): m/z = 430.3. ESI-HR-MS calculated for $C_{19}H_{22}$ FN_3O_4S (M^++H): 408.1393, found: 408.1391.

2-(4-methylphenylsulfonamido)-*N*-(1-(3-nitrophenylamino)-1-oxopropan-2-yl)propanamide (7j). Yield: 53%; a white solid, mp 173–175 °C; $R_f = 0.44$ (Hexane: EtOAc, 3:7, v/v).IR ($CHCl_3$) ν_{max}: 1246, 1346, 1433 (S=O), 1602, 1665 (C=O), 3340 (N–H) cm^{-1}.^{1}H NMR (400 MHz, DMSO-d_6): $\delta = 1.07$ (d, $J = 7.0$ Hz, 3H), 1.23 (d, $J = 7.0$ Hz, 3H), 2.37 (s, 3H), 3.86(p, $J = 7.2$ Hz, 1H), 4.21 (p, $J = 7.1$ Hz, 1H), 7.36 (d, $J = 8.1$ Hz, 2H), 7.59–7.69 (m, 3H), 7.88–7.93 (m, 3H), 8.19 (d, $J = 7.0$ Hz, 1H), 8.62 (t, $J = 2.1$ Hz, 1H), 10.43 (s, 1H). ^{13}C NMR (100 MHz, DMSO-d_6): 18.2, 19.4, 21.4, 49.5, 52.0, 113.7, 118.4, 125.6, 127.1, 129.8, 130.7, 138.7, 140.4, 143.1, 148.4, 171.6, 172.2 (C=O). MS (ESI + Na): m/z = 457.2. ESI-HR-MS calculated for $C_{19}H_{22}N_4O_6S$ (M^++H): 435.1338, found: 435.1331.

2-(4-methylphenylsulfonamido)-*N*-(1-oxo-1-(3-(trifluoromethyl) phenylamino)propan-2-yl)propanamide (7k). Yield: 71%; a white solid, mp 206–208 °C; $R_f = 0.52$ (Hexane: EtOAc, 3:7, v/v).IR ($CHCl_3$) ν_{max}: 1332, 1382 (S=O), 1645, 1691 (C=O), 3201, 3269, 3338 (N–H) cm^{-1}.^{1}H NMR (400 MHz, DMSO-d_6): $\delta = 1.07$ (d, $J = 7.0$ Hz, 3H), 1.22 (d, $J = 7.1$ Hz, 3H), 2.36 (s, 3H), 3.81–3.88 (m, 1H), 4.21 (p, $J = 7.1$ Hz, 1H), 7.35 (d, $J = 8.1$ Hz, 2H), 7.04 (d, $J = 7.8$ Hz, 1H), 7.55 (t, $J = 7.7$Hz, 1H), 7.68 (d, $J = 8.3$ Hz, 2H), 7.77 (d, $J = 8.4$ Hz, 1H), 7.92 (d, $J = 8.5$ Hz, 1H), 8.08 (s, 1H), 8.15 (d, $J = 7.1$ Hz, 1H), 10.27 (s, 1H). ^{13}C NMR (100 MHz, DMSO-d_6): 18.3, 19.4, 21.4, 49.4, 52.0, 115.6, 120.2, 123.2, 125.9, 127.1, 129.8, 130.1, 130.5, 138.6, 140.1, 143.0, 171.6, 171.9 (C=O). MS (ESI+): m/z = 458.4. ESI-HR-MS calculated for $C_{20}H_{22}F_3N_3O_4S$ (M^++H): 458.1361, found: 458.1357.

***N*-(3,4-dichlorophenyl)-2-(2-(4-methylphenylsulfonamido)propanamido)propanamide(7l)**. Yield: 75%; a white solid, mp 220–224 °C; $R_f = 0.48$ (Hexane: EtOAc, 3:7, v/v).IR ($CHCl_3$) ν_{max}: 1331, 1385 (S=O), 1638 (C=O), 3253, 3290 (N–H) cm^{-1}.^{1}H NMR (400 MHz, DMSO-d_6): $\delta = 0.99$ (d, $J = 7.1$ Hz, 3H), 1.13 (d, $J = 7.0$ Hz, 3H), 2.30 (s, 3H), 3.77(p, $J = 7.3$ Hz, 1H), 4.11 (p, $J = 7.1$ Hz, 1H), 7.28 (d, $J = 7.9$ Hz, 2H), 7.41 (dd, $J^1 = 8.9$; $J^1 = 8.9$ Hz; $J^2 = 2.4$ Hz, 1H), 7.50 (d, $J = 8.8$ Hz, 1H), 7.60 (d, $J = 8.3$ Hz, 2H), 7.84 (d, $J = 8.1$ Hz, 1H), 7.89 (d, $J = 2.4$ Hz, 1H), 8.08 (d, J = 7.1 Hz, 1H), 10.15 (s, 1H). ^{13}C NMR (100 MHz, DMSO-d_6): 18.3, 19.4, 21.4, 49.4, 51.9, 119.7, 120.8, 125.3, 127.1, 129.8, 131.2, 131.5, 138.6, 139.4, 143.0, 171.6, 171.9 (C=O). ESI-HR-MS calculated for $C_{19}H_{21}Cl_2N_3O_4S$ (M^++H): 458.0708, found: 458.0706.

***N*-(3-chloro-4-fluorophenyl)-2-(2-(4-methylphenylsulfonamido) propanamido)propanamide (7m)**. Yield: 68%; a white solid, mp 192–194 °C; $R_f = 0.55$ (Hexane: EtOAc, 3:7, v/v).IR ($CHCl_3$) ν_{max}: 1162, 1216, 1333 (S=O), 1640, 1675 (C=O), 3263, 3365 (N–H) cm^{-1}.^{1}H NMR (400 MHz, DMSO-d_6): $\delta = 1.05$ (d, $J = 7.0$ Hz, 3H), 1.20 (d, $J = 7.1$ Hz, 3H), 2.36 (s, 3H), 3.81 (p, J = 7.0 Hz, 1H), 4.18 (p, $J = 7.0$ Hz, 1H), 7.34–7.39 (m, 3H), 7.43–7.47 (m, 1H), 7.67 (d, J = 8.2 Hz, 2H), 7.88–7.92 (m, $J = 8.3$ Hz, 2H), 8.14 (d, $J = 7.4$ Hz, 1H), 10.14 (s, 1H). ^{13}C NMR (100 MHz, DMSO-d_6): 18.4, 19.4, 21.4, 49.3, 52.0, 117.3, 117.6, 119.5, 119.9, 121.0, 127.1, 129.8, 136.5, 138.6, 143.0, 171.5 (C=O). MS (ESI+): m/z = 442.3. ESI-HR-MS calculated for $C_{19}H_{21}$ $ClFN_3O_4S$ (M^++H): 442.1004, found: 442.1000.

***N*-(3,4-dimethoxyphenyl)-2-(2-(4-methylphenyl sulfonamido) propanamido) propanamide (7n)**. Yield: 57%; a light brown solid, mp 192–194 °C; $R_f = 0.37$ (Hexane: EtOAc, 1:9, v/v). IR ($CHCl_3$) ν_{max}: 1326, 1454(S=O), 1658 (C=O), 3349 (N–H) cm^{-1}.^{1}H NMR (400 MHz, DMSO-d_6): $\delta = 1.06$ (d, $J = 7.1$ Hz, 3H), 1.19 (d, $J = 7.1$ Hz, 3H), 2.37 (s, 3H), 3.72 (d, $J = 3.0$ Hz, 6H), 3.82 (p, $J = 7.2$ Hz,1H), 4.21(p, $J = 7.6$ Hz, 1H), 6.88 (d, $J = 8.8$ Hz, 1H), 7.09 (dd, $J^1 = 8.7$ Hz; $J^2 = 2.4$ Hz, 1H), 7.29 (d, J = 2.3 Hz, 1H), 7.36 (d, $J = 8.1$ Hz, 2H), 7.68 (d, $J = 8.3$ Hz, 2H), 7.93 (d, $J = 8.3$ Hz, 1H), 8.06 (d, $J = 7.3$ Hz, 1H), 9.77 (s, 1H). ^{13}C NMR (100 MHz, DMSO-d_6): 18.7, 19.4, 21.4, 49.2, 52.1, 55.9, 56.2, 104.9, 111.6, 112.6, 127.1, 129.9, 132.9, 138.5, 143.1, 145.4, 149.1, 170.7, 171.4 (C=O). ESI-HR-MS calculated for $C_{21}H_{27}N_3O_6S$ (M^++H): 450.1699, found: 450.1696.

***N*-(3,5-dimethylphenyl)-2-(2-(4-methylphenyl sulfonamido) propanamido) propanamide (7°)**. Yield: 44%; a white solid, mp 190–192 °C; $R_f = 0.44$ (Hexane: EtOAc, 3:7, v/v). IR ($CHCl_3$) ν_{max}: 1314, 1380 (S=O), 1635, 1681 (C=O), 3193, 3265, 3351(N–H) cm^{-1}.^{1}H NMR (400 MHz, DMSO-d_6): $\delta = 1.06$ (d, $J = 7.1$ Hz, 3H), 1.18 (d, $J = 7.1$ Hz, 3H), 2.17 (d, $J = 8.1$ Hz, 6H), 2.37 (s, 3H), 3.83 (p, $J = 7.1$ Hz,1H), 4.22 (q,$J = 7.2$ Hz, 1H), 7.04 (d, $J = 8.2$ Hz, 1H), 7.29 (d, $J = 8.1$ Hz, 1H), 7.36 (d, $J = 7.8$ Hz, 3H), 7.68 (d, $J = 8.31$ Hz, 2H), 7.92 (d, $J = 8.5$ Hz, 1H), 8.05 (d, $J = 7.4$ Hz, 1H), 9.75 (s, 1H). ^{13}C NMR (100 MHz, DMSO-d_6): 18.7, 19.2, 19.4, 20.1, 21.4, 49.2, 52.1, 117.2, 120.9, 127.1, 129.9, 130.1, 131.5, 136.8, 137.0, 138.6, 143.1, 170.9, 171.4 (C=O). MS (ESI+): m/z = 418.3. ESI-HR-MS calculated for $C_{21}H_{27}N_3O_4S$ (M^++H): 418.1801, found: 418.1796.

***N*-benzyl-2-(2-(4-methylphenylsulfonamido)propanamido)propanamide(7p)**. Yield: 65%; a white solid, mp 210–212 °C; R_f = 0.37 (Hexane: EtOAc, 3:7, v/v). IR ($CHCl_3$) ν_{max}: 1335, 1448 (S=O), 1639 (C=O), 3252, 3308 (N–H) cm^{-1}.^{1}H NMR (400 MHz, DMSO-d_6): δ = 1.04 (d, J = 7.0 Hz, 3H), 1.13 (d, J = 7.1 Hz, 3H), 2.37 (s, 3H), 3.76–3.83 (m, 1H), 4.01 (p, J = 7.1 Hz, 1H), 4.22–4.32 (m, 2H), 7.21–7.25 (m,3H), 7.29–7.36 (m,4H), 7.66 (d, J = 8.3 Hz, 2H), 7.91 (d, J = 8.4 Hz, 1H), 7.99 (d, J = 7.2 Hz, 1H), 8.32 (t, J = 5.9 Hz, 1H). ^{13}C NMR (100 MHz, DMSO-d_6): 18.7, 19.3, 21.4, 42.4, 48.6, 52.1, 127.1, 127.2, 127.5, 128.7, 129.9, 138.6, 139.7, 143.0, 171.3, 172.3 (C=O). MS (ESI+): m/z = 404.3. ESI-HR-MS calculated for $C_{20}H_{25}N_3O_4S$ (M^++H): 404.1644, found: 404.1640.

***N*-(4-chlorobenzyl)-2-(2-(4-methylphenylsulfonamido)propanamido)propanamide (7q)**. Yield: 48%; a white solid, mp 218–220 °C; R_f = 0.33 (Hexane: EtOAc, 3:7, v/v).IR ($CHCl_3$) ν_{max}: 1333, 1433 (S=O), 1634 (C=O), 3246, 3342, 3618, 3685 (N–H) cm^{-1}.^{1}H NMR (400 MHz, DMSO-d_6): δ = 1.04 (d, J = 7.0 Hz, 3H), 1.13 (d, J = 7.0 Hz, 3H), 2.38 (s, 3H), 3.75–3.83 (m, 1H), 4.08(p, J = 7.1 Hz, 1H), 4.20–4.30 (m, 2H), 7.24 (d, J = 8.5 Hz, 2H), 7.34–7.37 (m,4H), 7.66 (d, J = 8.2 Hz, 2H), 7.90 (d, J = 8.4 Hz, 1H), 8.01 (d, J = 7.3 Hz, 1H), 8.35 (t, J = 6.0 Hz, 1H). ^{13}C NMR (100 MHz, DMSO-d_6): 18.6, 19.3, 21.4, 41.8, 48.6, 52.1, 127.1, 128.7, 129.3, 129.8, 131.7, 138.6, 138.8, 143.0, 171.4, 172.4 (C=O). MS (ESI + Na): m/z = 460.2. ESI-HR-MS calculated for $C_{20}H_{25}ClN_3O_4S$ (M^++H): 438.1254, found: 438.1250.

***N*-(4-fluorobenzyl)-2-(2-(4-methylphenylsulfonamido)propanamido)propanamide(7r)**. Yield: 44%; a white solid, mp 219–221 °C; R_f = 0.35 (Hexane: EtOAc, 3:7, v/v).IR ($CHCl_3$) ν_{max}: 1331, 1385 (S=O), 1638 (C=O), 3253, 3290 (N–H) cm^{-1}.^{1}H NMR (400 MHz, DMSO-d_6): δ = 1.04 (d, J = 7.0 Hz, 3H), 1.13 (d, J = 7.0 Hz, 3H), 2.38 (s, 3H), 3.79(p, J = 7.0 Hz, 1H), 4.08 (p, J = 7.2 Hz, 1H), 4.20–4.29 (m, 2H), 7.10–7.16 (m,2H), 7.24–7.27 (m,2H), 7.35 (d, J = 8.0 Hz, 2H), 7.66 (d, J = 8.3 Hz, 2H), 7.91 (d, J = 7.2 Hz, 1H), 8.00 (d, J = 7.3 Hz, 1H), 8.3 (t, J = 5.91 Hz, 1H). ^{13}C NMR (100 MHz, DMSO-d_6): 18.6, 19.3, 21.4, 41.7, 48.6, 52.1, 115.3, 115.5, 127.1, 129.4, 129.5, 129.9, 135.9, 138.6, 143.0, 171.4, 172.3 (C=O). ESI-HR-MS calculated for $C_{20}H_{24}FN_3O_4S$ (M^++H): 422.1550, found: 422.1547.

2-(4-methylphenylsulfonamido)-*N*-(1-oxo-1-(4-(trifluoromethyl) benzylamino)propan-2-yl) propanamide (7s). Yield: 57%; a white solid, mp 231–233 °C; R_f = 0.34 (Hexane: EtOAc, 3:7, v/v). IR ($CHCl_3$) ν_{max}: 1216, 1331, 1378 (S=O), 1641 (C=O), 3252, 3299 (N–H) cm^{-1}.^{1}H NMR (400 MHz, DMSO-d_6): δ = 1.04 (d, J = 7.0 Hz, 3H), 1.15 (d, J = 7.1 Hz, 3H), 2.38 (s, 3H), 3.80 (p, J = 7.3 Hz, 1H), 4.10(p, J = 7.1 Hz, 1H), 4.30–4.40 (m, 2H), 7.35 (d, J = 8.0 Hz, 2H), 7.44 (d, J = 8.0 Hz, 2H), 7.66–7.72 (m, 4H), 7.91 (d, J = 8.3 Hz, 1H), 8.03 (d, J = 7.3 Hz, 1H), 8.45 (t, J = 6.0 Hz, 1H). ^{13}C NMR (100 MHz, DMSO-d_6): 18.5, 19.3, 21.4, 48.7, 52.1, 125.6, 126.1, 127.1, 127.2, 127.8, 128.1, 129.8, 138.6, 143.0, 144.7, 171.4, 172.6 (C=O). ESI-HR-MS calculated for $C_{21}H_{24}N_3O_4S$ (M^++H): 472.1518, found: 472.1512.

2-(4-methylphenylsulfonamido)-*N*-(1-(naphthalen-1-ylamino)-1-oxopropan-2-yl)propanamide (7t). Yield: 31%; a light brown solid, mp 202–204 °C; R_f = 0.57 (Hexane: EtOAc, 3:7, v/v). IR ($CHCl_3$) ν_{max}: 1337, 1439 (S=O), 1633 (C=O), 3256, 3296, 3343, 3619, 3685 (N–H) cm^{-1}.^{1}H NMR (400 MHz, DMSO-d_6): δ = 1.09 (d, J = 7.0 Hz, 3H), 1.32 (d, J = 7.1 Hz, 3H), 2.38 (s, 3H), 3.88(p, J = 7.7 Hz,1H), 4.45(p, J = 6.9 Hz, 1H), 7.37 (d, J = 8.1 Hz, 2H), 7.48–7.56 (m, 3H), 7.62–7.71 (m, 3H), 7.78 (d, J = 8.2 Hz, 1H), 7.93–8.02 (m,3H), 8.19 (d, J = 7.1 Hz, 1H), 9.91 (s, 1H). ^{13}C NMR (100 MHz, DMSO-d_6): 18.6, 19.4, 21.4, 49.2, 52.1, 122.3, 123.1, 126.0, 126.4, 126.5, 127.1, 128.4, 128.6, 129.9, 133.6, 134.2, 138.7, 143.1, 171.7, 172.0 (C=O). MS (ESI+): m/z = 440.3. ESI-HR-MS calculated for $C_{21}H_{27}N_3O_4S$ (M^++H): 440.1644, found: 440.1641.

2-(4-methylphenylsulfonamido)-N-(1-(5-methylthiazol-2-ylamino)-1-oxopropan-2-yl)propanamide (7u). Yield: 73%; a white solid, mp 204–206 °C; R_f = 0.42 (Hexane: EtOAc, 3:7, v/v).IR ($CHCl_3$) ν_{max}: 1308, 1384 (S=O), 1656, 1688 (C=O), 3195 (N–H) cm^{-1}.^{1}H NMR (400 MHz, DMSO-d_6): δ = 1.05 (d, J = 7.1 Hz, 3H), 1.18 (d, J = 7.2 Hz, 3H), 2.33 (s, 3H),2.36 (s, 3H), 3.81–3.88 (m, 1H), 4.25 (p, J = 7.1 Hz, 1H), 7.12 (d, J = 1.2 Hz, 1H), 7.34 (d, J = 8.1 Hz, 2H), 7.66 (d, J = 8.2 Hz, 2H), 7.89 (d, J = 9.1 Hz, 1H), 8.14 (d, J = 6.9 Hz, 1H), 11.92 (s, 1H). ^{13}C NMR (100 MHz, DMSO-d_6): 11.5, 18.2, 19.4, 21.4, 48.5, 51.9, 126.9, 129.8, 135.2, 138.7, 143.0, 156.4, 171.1, 171.5 (C=O). MS (ESI+): m/z = 411.4. ESI-HR-MS calculated for $C_{17}H_{22}$ $N_4O_4S_2$(M^++H): 411.1161, found: 468.1158.

***N*-(benzo [d] thiazol-2-yl)-2-(2-(4-methylphenylsulfonamido) propanamido)propanamide (7v)**. Yield: 84%; a white solid, mp 248–250 °C; R_f = 0.56 (Hexane: EtOAc, 3:7, v/v).IR ($CHCl_3$) ν_{max}: 1260, 1310, 1440 (S=O), 1643 (C=O), 3249, 3298 (N–H) cm^{-1}.^{1}H NMR (400 MHz, DMSO-d_6): δ = 1.08 (d, J = 7.0 Hz, 3H), 1.25 (d, J = 7.2 Hz, 3H), 2.37 (s, 3H), 3.88 (p, J = 7.3 Hz, 1H), 4.31 (p,J = 7.0 Hz, 1H), 7.29–7.37 (m, 3H), 7.42–7.46 (m, 1H), 7.68 (d, J = 8.3 Hz, 2H), 7.75 (d, J = 8.0 Hz, 1H), 7.92 (d, J = 8.7 Hz, 1H), 7.97 (d, J = 7.8 Hz, 1H),8.24 (d, J = 6.4 Hz, 1H), 12.40 (s, 1H). ^{13}C NMR (100 MHz, DMSO-d_6): 17.9, 19.4, 21.4, 48.9, 51.8, 121.0, 122.2, 124.1, 126.6, 127.1, 129.8, 131.9, 138.7, 143.0, 149.0, 158.3, 171.6, 172.5 (C=O). MS (ESI+): m/z = 447.3. ESI-HR-MS calculated for $C_{20}H_{22}N_4O_4S_2$(M^++H): 447.1161, found: 447.1158.

***N*-(adamantan-1-yl)-2-(2-(4-methylphenylsulfonamido)propanamido)propanamide (7w)**. Yield: 61%; a white solid, mp 223–225 °C; R_f = 0.53 (Hexane: EtOAc, 3:7, v/v).IR ($CHCl_3$) ν_{max}: 1161, 1216, 1384 (S=O), 1657 (C=O), 3394 (N–H) cm^{-1}.^{1}H NMR (400 MHz, DMSO-d_6): δ = 1.04 (dd, J^1 = 15.2 Hz; J^2 = 6.9 Hz, 6H),1.61 (s, 6 H), 1.89 (s, 6H), 2.00 (s, 3H), 2.38 (s, 3H), 3.75 (p, J = 7.7 Hz, 1H), 4.04 (p, J = 7.4 Hz, 1H), 7.23 (s, 1H), 7.36 (d, J = 8.1 Hz, 2H), 7.67 (d, J = 8.1 Hz, 2H), 7.81 (d, J = 7.5 Hz, 1H), 7.92 (d, J = 8.4 Hz, 1H). ^{13}C NMR (100 MHz, DMSO-d_6): 19.2, 19.3, 21.4, 29.2, 36.4, 41.4, 48.7, 51.1, 52.2, 127.1, 130.0, 138.5, 143.1, 171.1, 171.4 (C=O). MS (ESI+): m/z = 448.4. ESI-HR-MS calculated for $C_{23}H_{33}N_3O_4S$ (M^++H): 448.2270, found: 448.2266.

2.3. Screening for in vitro P. falciparum activity

The sample concentration that inhibits the growth of chloroquine sensitive strains of *P. falciparum* development by 50% (IC_{50}) was measured and used to determine the antimalarial potencies of the new derivatives as thus: Sorbitol synchronized, 0.1% parasitemia, ring stage P. falciparum strain W2 parasites were cultured under the atmosphere of 3% O_2, 6% CO_2 and 91% N2 in RPMI-1640 medium supplemented with 10% human serum in the presence of inhibitors for 48 h without media change. Inhibitors were added from 1000 x DMSO stocks. After 48 h, the culture medium was removed and replaced with 1% formaldehyde in PBS pH 7.4 for an additional 48 h at room temperature to fix cells. Fixed parasites were transferred into 0.1% Triton-X-100 in PBS containing 1 nM YOYO-1 dye (Molecular Probes). Parasitemia was determined from dot plots (forward scatter vs. fluorescence) acquired on a FACS sort flow cytometer using Cell Quest software (Beckton Dickinson).

2.4. In vitro antioxidant assay

The ability of the new dipeptides to reduce the 2,2-diphenyl-1-picrylhydrazyl (DPPH) radical was used to assess their antioxidant effect. Different test tubes containing solutions of each of the compounds in different concentrations (5, 10, 15, 20, and 25 μg/mL) were prepared in DMSO. 1 mL of freshly prepared DPPH solution (0.004 % w/v) was added into each of these test tubes and shaken to mix properly. The test tubes were allowed to incubate in the dark room temperature for 30 min. A blank solution containing everything else in the sample solution except the test compounds was also prepared and DPPH was used for the baseline correction. UV-Visible spectrometer was used to take record absorbance at 517 nm against the blank solution. Percentage inhibition (PI) of DPPH radical activity was used to measure the radical scavenging activities of the dipeptides [28].

DPPH radical scavenging activity (%) = $[(A_{DPPH} - A_{sample})/A_{DPPH}]$* 100

Where A_{DPPH} = absorbance of control and A_{sample} = absorbance of samples/ascorbic acid.

2.5. Homology modeling

The PfNMT homology model was built using modeller v 9.21 [29] using the PfNMT sequence (accession number: AAF18461.1) as a query sequence and X-ray crystal structure of *P. vivax* NMT in complex with the cofactor and inhibitor (accession number: 2YND) as a template [30]. Sequence-identity and –similarity were used to check the suitability of the template. The best model was selected out of 20 homology models of PfNMT based on the evaluation by the Modeller objective function and Discrete Optimized Protein Energy profile. Gromos force field 53a6 in Gromacs was used to energy minimize the selected model before using Discovery Studio module for Ramanchandran plots to evaluate the model quality [31].

2.6. Generating models of the toluene-sulphonamide dipeptides

The 3-D structure of the newly synthesized dipeptides were generated using the graphical user interface module in molecular operating environment (MOE) and MMFF94 force field module in MOE was used to energy minimize them to an energy gradient of 0.001 kcal/mol. Also. Some molecular descriptors used to assess drug-likeness (molecular weight (MW), lipophilicity (logP), hydrogen bond acceptor/donor (HBA and HBD)) of compounds were computed using QuSAR module implemented in MOE software [32].

2.7. Docking

The AutoDock4.2 program (Morris et al. 1998) was used to dock the dipeptides into the peptide-substrate binding domain of the PfNMT homology model. A grid box having 40 × 40 × 40 dimensions with 0.375 Å point spacing was centered in the mass center of -25.835, 14.762, -25.529 was built to cover the reference ligand (a pyrazole sulfonamide). All other AutoDockTool parameters were kept as default except for the rmsd tolerance that was set at 2.00 Å and number of rotatable bonds at maximum of 6.

3. Results and discussion

3.1. Synthesis and characterization of new dipeptide-sulphonamide derivatives

The synthesis of the sulfonamide dipeptides is outlined in Scheme 1. Zhan and co-workers explained that toluene sulfonyl moiety is optimal to the antimalarial activity asparagine ethylene diamine in the culture *P. falciparum* [16]. The reaction between toluenesulfonyl chloride **1a** and alanine in the presence of sodium carbonate afforded the sulphonamide **3**. The activation reaction of Boc-alanine **4a** with amine gave compound **5** which after deprotection provided compound **6**. The cross-coupling reaction of compound **3** with **6** via 1-ethyl-3-(3-dimethylaminopropyl) carbodiimide HCl (EDC) in the presence of 1-hydroxybenzotriazole (HOBt) afforded the 'ala-ala' dipeptide sulfonamides in good yields (**7a-7w**). The compounds were fully characterized by combine FTIR, ^{1}H, ^{13}C spectroscopy and MS analyses (Supporting Information) and were found to be in agreement with their proposed structures and molecular formulas. The IR bands for the N–H, C=O and S=O groups were found within the range of 3400–3200, 1600–1800 and 1200–1400 nm respectively. While the methyl protons absorption signals of toluenesulfonyl moieties appeared as singlets around 2.37 ppm, the two methyl groups between the phenyl rings at both ends of the derivatives appeared as doublets around 1.06 ppm and 1.20 ppm in the compounds (**7a-7w**) apparently due to splitting by one hydrogen atom. The more deshielded

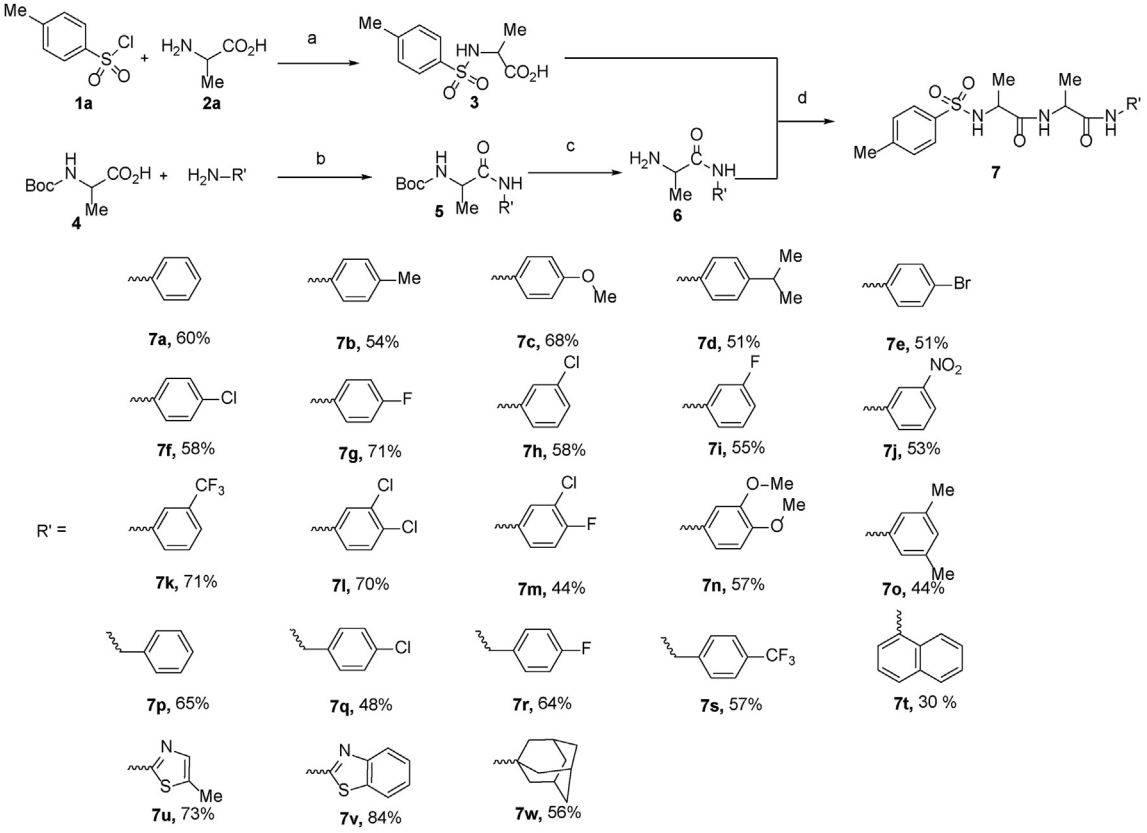

Scheme 1. Synthesis of toluenesulfonamidedipeptide, *Reagents and Conditions*- (a) Na_2CO_3, 0 °C - rt, 6 h; (b) EDC.HCl, HOBt, DIPEA, DCM, rt, 18 h; (c) DCM/TFA (1:1 v/v); (d) EDC.HCl, HOBt, DIPEA, DCM, rt, 18 h.

two ortho O-methyl substituents chemical shifts (3.72 ppm) of the anilino ring of compound **7n** appeared at lower field than the two *meta* methyl substituents of the anilino ring of compound **7o**. The aromatic protons of the two phenyl rings at both end of the molecules appeared within 6.88–7.68 ppm while the N–H protons appeared at much higher frequency ranges in the spectra of the compounds. In addition, benzylic proton signals integrated as multiplets for two protons for compounds (**7p-7s**).

The ^{13}C NMR spectra conspicuously furnished the chemical shifts of the carbonyl carbons at around 171.0–172.0 ppm. All other spectral data including the HRMS confirmed the molecular structures of the compounds (supporting document attached). All the synthesised target compounds possess purity of between 98 -100% in HPLC.

3.2. Drug-like profile

Many compounds with high pharmacological activities have failed to succeed as drugs due to bad physicochemical properties. That is why basic physicochemical features, such as drug-likeness, of potential drug candidates are assessed at early stage of drug development to avoid resource wastage on bad candidate [33, 34]. Molecules which have molecular weight (MW), lipophilicity (logP), hydrogen bond acceptor/donor (HBA and HBD) in the respective ranges of $\leq$500 Da, $\leq$ 5, $\leq$10 and $\leq$5 as a rule of thumb are found to be orally bioavailable in systemic circulation. This originated from the research conducted by Lipinski in which he discovered that more than 90% of approved drugs with good drug-like profile possess the stated properties [35, 36]. These criteria are used to screen putative drugs to avoid wasting time and money on wrong candidate. Except for **7q** (MW = 514.04 Da) and **7s** (MW = 547.59 Da) that have more than 500 Da, results of all the computed molecular descriptors for each of the dipeptide fall within the recommended region for druglikeness (Table 1). This result suggests that the new compounds will likely not pose any pharmacokinetic challenge and therefore are worthy drug candidates.

3.3. In-vitro biological testing and evaluation of the structure-antiplasmodium activity relationship

Activities of the newly synthesised dipeptides against chloroquine sensitive 3D7 strain of *P. falciparum* were investigated and results are shown in Table 2. Overall it was observed that the derivatives with substituent benzyl ring at the N-terminal position bearing either fluorine or chlorine at meta or para or both positions (**7f-7i, 7l, 7m, 7q, 7r**) demonstrated higher activities against the parasite than their counterparts with alkyl, bromine or methoxyl group. Moreover, attempt to replace fluorine or chlorine with bromine or methoxyl group led to complete loss of activity (**7c, 7e** and **7n**). In addition, it appears that the probed N-terminal position does not tolerate completely nonpolar rigid moieties (**7a**, **7p** and **7t**) because compound **7v** (IC_{50} = 4.00 μM), with rigid substituent bearing polar heteroatoms, resulted in antiplasmodial activity being remarkably restored. Compound **7w** (IC_{50} = 3.60 μM) took an exception from the later observation. Probably, something about the stereochemistry of the substituent residue enhanced its activity. Although, the activities shown by the new derivatives do not compare to the reference drug, chloroquine (IC_{50} = 0.06 μM), and the difference between the most and least potent dipeptide derivatives suggests there is a flat structure-activity relationship (SAR), analysis of their SAR could give hints to the structural features of the substituents at N-terminal position required for antiplasmodial activity which could be vital for further structure-activity optimization.

In view of the damages free radicals cause to healthy cells, compounds having antiplasmodial activity and can reduce/neutralize free radicals are of double advantage. The free DPPH radical scavenging ability of derivatives **7h**, **7m** and **7n**, having single digit IC_{50} values of 7.53, 7.21 and 6.01 μg/mL respectively, were comparable to that of ascorbic acid (IC_{50} = 1.06 μg/mL) as represented in Table 2. In general, the antioxidant activities of the derivatives ranged from 6.01 – 13.51 μg/mL and all the dipeptides were able to reduce more than 50% of the free radical at 15 μg/mL. It is worthy to note that **7h** and **7m** compounds

Table 1. Calculated molecular descriptors used to predict drug-likeness.

Compound codes	HBA	HBD	logP (o/w)	MW(Da)
7a	7	3	2.13	389.47
7b	7	3	2.42	403.50
7c	8	3	2.08	419.50
7d	10	2	1.89	478.50
7e	7	3	2.92	468.37
7f	10	2	2.39	498.91
7g	7	3	2.28	407.46
7h	7	3	2.76	423.92
7i	7	3	2.32	407.46
7j	10	3	2.10	434.47
7k	7	3	3.10	457.47
7l	7	3	3.35	458.36
7m	7	3	2.91	441.91
7n	9	3	1.82	449.52
7o	7	3	2.83	417.53
7p	7	3	4.17	479.60
7q	7	3	4.77	514.04
7r	7	3	4.33	497.59
7s	7	3	4.81	547.59
7t	7	3	3.35	439.53
7u	8	3	1.28	410.51
7v	8	3	2.75	446.55
7w	7	3	2.90	447.60

Table 2. *In vitro* anti-*P. falciparum* activities against chloroquine sensitive 3D7 strain of *P. falciparum* and anti-oxidant activities of the compounds[#].

Compound codes	Anti-*P. falciparum* activity IC_{50} (μM)	Anti-oxidant activity (DPPH) IC_{50} (μg/mL)
7a	na	10.57
7b	17.10	11.94
7c	na	12.07
7d	15.20	12.06
7e	na	12.62
7f	4.60	12.93
7g	5.00	12.93
7h	6.00	7.53
7i	4.20	12.58
7j	8.00	12.01
7k	**3.80**	11.97
7l	4.60	12.72
7m	**3.20**	**7.21**
7n	na	6.01
7o	na	11.02
7p	na	13.51
7q	13.60	12.05
7r	8.20	11.91
7s	9.10	12.95
7t	na	12.39
7u	4.60	12.84
7v	**4.00**	12.29
7w	**3.60**	12.98
Chloroquine	0.06	-
Ascorbic acid	-	1.06

#Most active compounds are bolded.

maintained relatively remarkable distinct antiplasmodial and antioxidant potencies. Hence, aside being able to inhibit *P. falciparum* growth these derivatives can also protect cells and membranes from the harmful effects of free radicals which might have been produced from pathogenic mechanism of the parasite.

3.4. Homology modelling

Since the 3-dimensional structure of NMT from *P. falciparum* was not available in protein databank (PDB), modeller v 9.21 was used to construct the homology model of PfNMT in complex with the cofactor (myristoyl CoA) and the X-ray crystal structure of NMT from *P. vivax* in complex with the cofactor and an inhibitor, a pyrazole sulfonamide (PDB code: 2YND) as a template. Target and template showed sequence-identity and -similarity of 82% and 93% respectively. The root mean square deviation (rsmd) computed from the alignment of the PfNMT homology model and PvNMT retrieved from protein databank was found to be 0.350 Å. The Ramanchandran plot of the PfNMT homology model (Figure 1) confirmed that the model is of good stereochemical quality.

3.5. Docking calculation

AutoDock4.2 was used to perform docking of the ligands into the peptide-substrate binding domain of the PfNMT homology model. The peptide binding site of PfNMT homology model predicted by Site-Finder protocol in MOE tallied with the position suggested by superimposition of the template-protein in complex with the reference ligand. The ability of the docking program to reproduce ligand poses comparable to that of X-ray crystallography within root mean square deviation tolerance of 2 Å was used to check the reliability of the dock workflow. Through visual inspection it can be inferred that the conformations of the reference ligand as shown in Figure 2 clearly demonstrates that retained docking protocol is satisfactory. Rigid-protein-flexible-ligand docking scheme was employed to dock the twenty-three new derivatives towards the PfNMT homology model and the calculated free energy of binding, inhibition constant and ligand efficiency obtained show that all the dipeptides favourably interacted with PfNMT within the peptide binding pocket (Table 3). Compounds **7e**, **7q**, **7t** and **7w** have K_i at sub-micromolar ranges (K_i = 0.72, 0.75, 0.57, and 0.53 μM respectively) that are comparable to the reference ligand (a pyrazole sulfonamide; K_i = 0.01 μM) while the rest have single digit micromolar values except for **7k**

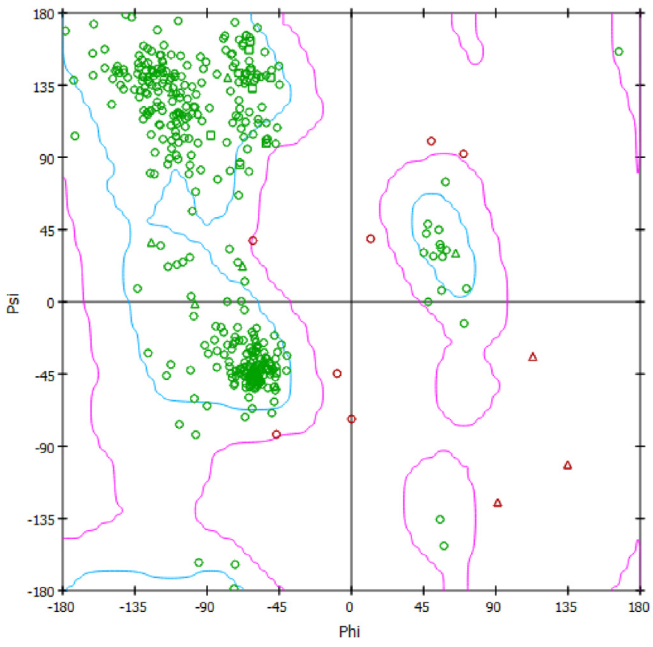

Figure 1. The Ramanchandran plot of the PfNMT homology model.

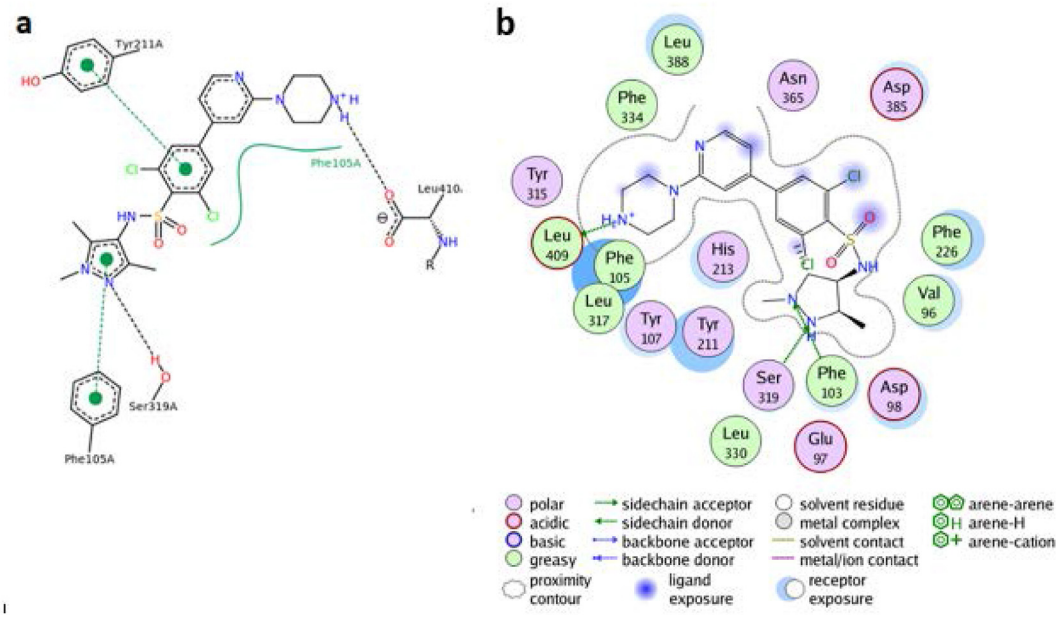

Figure 2. The reference ligand i.e. the pyrazole sulphonamide (a) X-ray crystallography predicted binding pose in *P. vivax* NMT and (b) docked pose predicted by AutoDock4.2v in the PfNMT homology model.

Table 3. Docking results of the compounds towards *P. falciparum* N-myristoyl transferase homology model.

Compound codes	Free binding energy (kcal/mol)	Inhibition constant K_i (μM)	Ligand efficiency
7a	-7.47	3.36	0.28
7b	-7.53	3	0.27
7c	-7.27	4.67	0.25
7d	-7.29	4.50	0.22
7e	**-8.38**	**0.72**	**0.3**
7f	-7.82	1.85	0.24
7g	-7.24	4.89	0.26
7h	-6.93	8.33	0.25
7i	-6.95	8.10	0.25
7j	-7.15	3.58	0.25
7k	-6.24	26.73	0.2
7l	-7.40	3.78	0.26
7m	-7.43	3.58	0.26
7n	-6.18	29.51	0.2
7o	-7.98	1.41	0.21
7p	-7.76	2.03	0.23
7q	**-8.36**	**0.75**	**0.24**
7r	-7.70	2.27	0.22
7s	-7.15	5.69	0.19
7t	**-8.52**	**0.57**	**0.27**
7u	-7.06	6.70	0.26
7v	-7.69	2.30	0.26
7w	**-8.56**	**0.53**	**0.28**
Reference ligand	-10.91	0.01	0.33

The compounds are in submicromolar ranges compared to the reference ligand and therefore more active amongst the ones considered.

and **7n** with double digit values (K_i = 26.73 and 29.51 μM). None of the dipeptides has ligand efficiency lower than 2.0 which putatively indicates ability of the derivatives to produce physiological change upon binding to PfNMT. Although each of the considered compounds has binding affinity for the protein target, only compound **7w** deserves further attention not only because of its high binding affinities, nor reasonable ligand efficiencies and drug-like character; but due to the fact that PfNMT inhibition is relatively a novel mechanism of antimalarial drug action. Moreover and importantly, **7w** has shown relative interesting antiplasmodial and antioxidant activities.

4. Conclusion

We have described the synthesis and complete characterization of new series of toluenesulfonamide dipeptide molecules. Their *in vitro* activities against chloroquine sensitive 3D7 strain of *P. falciparum* and

DPPH free radical provided important structure-activity relationship worthy of further effort to optimise activity of the synthesized derivatives. Compound **7w** demonstrated relatively better antiplasmodial activity uncommon for derivatives bearing similar substituent groups. We identified compounds **7h** and **7m** as the most interesting candidates because they showed distinct antiplasmodial and antioxidant potencies respectively. From molecular docking all the newly synthesised compounds were found to exhibit favourable binding interactions with PfNMT homology model. Moreover, out of four derivatives with theoretical K_i at submicromolar concentrations, compound **7m** stood out and worthy of further study because of its interesting dual antimalarial and antioxidative activities.

Declarations

Author contribution statement

Efeturi Onoabedje: Conceived and designed the experiments; Performed the experiments; Analyzed and interpreted the data; Wrote the paper.

Akachukwu Ibezim: Analyzed and interpreted the data; Wrote the paper.

Uchechukwu C. Okoro: Conceived and designed the experiments.

Sanjay Batra: Analyzed and interpreted the data; Contributed reagents, materials, analysis tools or data.

Funding statement

Efeturi Onoabedje was supported by India and Council of Scientific and Industrial Research, India and The World Academy of Science (TWAS).

Competing interest statement

The authors declare no conflict of interest.

Additional information

Supplementary content related to this article has been published online at https://doi.org/10.1016/j.heliyon.2020.e04958.

References

[1] A. Nzila, M. Zhenkun, K. Chibale, Drug repoposing in the treatment of malaria and TB, Future Med. Chem. 11 (3) (2011) 1414.
[2] A. Nzila, The Past, present and the future of antifolates in treatment of *plasmodium falciparum* infection, J. Antimicrob. Chemother. 57 (2006) 1045.
[3] P.A. Onguéné, F. Ntie-Kang, J.A. Mbah, L.L. Lifongo, J.C. Ndom, W. Sippl, L.M. Mbaze, The potential of anti-malarial compounds derived from African medicinal plants, part III: an *in silico* evaluation of drug metabolism and pharmacokinetics profiling, Org. Med. Chem. Lett. 4 (2013) 6.
[4] J. Ngo-Hanna, F. Ntie-Kang, M. Kaiser, R. Brun, S.M.N. Efange, 1-Aryl-1,2,3,4-tetrahydroisoquinolines as potential antimalarials: synthesis, *in vitro* antiplasmodial activity and *in silico* pharmacokinetics evaluation, RSC Adv. 4 (2014) 22856–22865.
[5] WHO Media Center, Fact Sheet on Malaria, 2020. https://www.who.int/en/news-room/fact-sheets/detail/malaria. (Accessed 4 April 2020).
[6] G. Ramakrishnan, N. Chandra, N. Srinivasan, Exploring antimalarial potential of FDA approved drugs: an in silico approach, Malar. J. 16 (290) (2017) 2.
[7] E.A. Ashley, A.P. Phyo, Drugs in development for malaria, Drugs 78 (2018) 861–879.
[8] E.G. Tse, M. Korsik, M.H. Todd, The past, present and future of antimalarial medicines, Malar. J. 18 (93) (2019) 1–21.
[9] N. Vale, L. Aguiar, P. Gomes, Antimicrobial peptides: a new class of antimalarial drugs? Front. Pharmacol. 5 (275) (2014) 1–13.
[10] L. Perez-Picaso, H.F. Olivo, R. Argotte-Ramos, M. Rodriguez-Gutierrez, M.Y. Rios, Linear and cyclic dipeptides with antimalarial activity, Bioorg. Med. Chem. Lett (2012) 7048–7051.
[11] A. Mahindra, R.P. Gangwal, S. Bansal, N.E. Goldfarb, B.M. Dunn, N.E. Sangamwar, R. Jain, Antiplasmodial activity of short peptide-based compounds, RSC Adv. (2015) 22674–22684.
[12] A. Bell, Antimicrobial peptides: the long and the short of it, Curr. Pharmaceut. Des. 17 (2011) 2719–2731.
[13] N. Bugday, F.Z. Kucukbay, H. Kucubay, S. Bua, G. Bartolucci, J. Leitans, A. Kazaks, K. Tars, C.T. Supuran, Synthesis and evaluation of novel benzimidazole conjugates incorporating amino acids and dipeptide moieties, Lett. Org. Chem. 14 (2017) 198–206.
[14] S.S. Panda, M.A. İbrahim, H. Küçükbay, M.J. Meyers, F.M. Sverdrup, A.A. El-Feky, A.R. Katritzky, Synthesis and antimalarial bioassay of quinine-peptide conjugates, Chem. Biol. Drug Des. 82 (2013) 361–366.
[15] M.A. Ibrahim, S.S. Panda, A.A. Oliferenko, P.V. Oliferenko, A.S. Girgis, M. Elagawany, F.Z. Küçükbay, C.S. Panda, G.G. Pillai, A. Samir, K. Tämm, C.D. Hall, A.R. Katritzky, Macrocyclic peptidomimetics with antimicrobial activity: synthesis, bioassay, and molecular modeling studies, Org. Biomol. Chem. 13 (2015) 9492–9503.
[16] W. Zhan, J. Visone, T. Ouellette, J.C. Harris, R. Wang, H. Zhang, P.K. Singh, J. Ginn, G.D. Sukenick, T.T. Wong, J.I. Okoro, R.M. Scales, P.T. Tumwebaze, P.J. Rosenthal, B.F.C. Kafsack, R. Cooper, P.T. Meinke, L.A. Kirkman, G. Lin, Improvement of asparagines ethylenediamines as antimalarial plasmodium-selective proteasome inhibitors, J. Med. Chem. 62 (2019) 6137–6138.
[17] J. Tang, H. Chen, Y. He, W. Sheng, Q. Bai, H. Wang, Peptide-guided functionalization and macrocyclization of bioactive peptidosulfonamides by Pd(II)-catalyzed late-stage C– H activation, Nat. Commun. 9 (2018) 3383.
[18] A. Pabon, J. Carmona, L.C. Burgos, S. Blair, Oxidative stress in patients with noncomplicated malaria, Clin. Biochem. 36 (2003) 71–78.
[19] K.R. Shankar, N.S.R. Kumari, G.V.N. Kiranmyi, In vitro study of antioxidant and antimalaria activities of new chromeno-pyrano-chromene derivative, Am. J. Phytomed. Clin. Ther. 2 (10) (2014) 1169–1176.
[20] I.A. Clark, N.H. Hunt, Evidence for reactive oxygen intermediates causing hemolysis and parasite death in malaria, Infect. Immun. 39 (1) (1983) 1–6.
[21] P.G. Kremsner, B. Greve, B. Lell, D. Luckner, D. Schmid, Malarial anaemia in African children associated with high oxygen-radical production, Lancet 355 (9197) (2000) 40–41.
[22] M. Guha, S. Kumar, V. Choubey, P. Maity, U. Bandyopadhyay, Apoptosis in liver during malaria: role of oxidative stress and implication ofmitochondrial pathway, Faseb. J. 20 (8) (2006) E439–E449.
[23] D.I. Ugwu, U.C. Okoro, P.O. Ukoha, S. Okafor, A. Ibezim, N.M. Kumar, Synthesis, characterization, molecular docking and in vitro antimalarial properties of new carboxamides bearing sulphonamide, Eur. J. Med. Chem. 135 (2017) 349–369.
[24] D.I. Ugwuja, U.C. Okoro, S.S. Soman, R. Soni, S.N. Okafor, D.I. Ugwu, New peptide derived antimalaria and antimicrobial agents bearing sulphonamide moiety, J. Enzym. Inhib. Med. Chem. 34 (1) (2019) 1388–1399.
[25] M.H. Wright, B. Clough, M.D. Rackham, K. Ranganchari, J.A. Brannigan, M. Grainger, D.K. Moss, A.R. Bottrill, W.P. Heal, M. Broncel, R.A. Serwa, D. Brady, D.J. Mann, R.J. Leatherbarrow, R. Tewari, A.J. Wilkinson, A.A. Holder, E.W. Tate, Validation of *N*-myristoyltransferase as an antimalarial drug target using an integrated chemical biology approach, Nat. Chem. 6 (2014) 112–121.
[26] C. Moskes, P.A. Burghaus, B. Wernli, U. Sauder, M. Durrenberger, B. Kappes, Export of *Plasmodium falciparum* calcium-dependent protein kinase 1 to the parasitophorous vacuole is dependent on three N-terminal membrane anchor motifs, Mol. Microbiol. 54 (2004) 676–691.
[27] R.R. Rees-Channer, S.R. Martin, J.L. Green, P.W. Bowyer, M. Grainger, J.E. Molloy, Dual acylation of the 45 kDa gliding-associated protein (GAP45) in Plasmodium falciparum merozoites, Mol. Biochem. Parasitol. 149 (2006) 113–116.
[28] R. Sutharsingh, S. Kavimani, B. Jayakar, M. Uvarani, A. Thangathirupathi, Quantitative phytochemical and antioxidant studies on aerial parts of Naravelia zeylanica DC, Int J Pharm Studies Res 2 (2) (2011) 52–56.
[29] M.A. Marti-Renom, A.C. Stuart, A. Fisemartir, R. Sanchez, F. Melo, A. Sali, Comparative protein structure modelling of genes and genomes, Annu. Rev. Biophys. Biomol. Struct. 29 (2000) 291–325.
[30] H.M. Berman, J. Westbrook, Z. Feng, G. Gilliland, T.N. Bhat, H. Weissig, I.N. Shindyalov, P.E. Bourne, The protein data bank, Nucleic Acids Res. 28 (2001) 235–342.
[31] R.P. Scott, P.H. Hunenberger, I.G. Tironi, A.E. Mark, S.R. Billeter, J. Fennen, A.E. Torda, T. Huber, P. Kruger, W.F. vanGunsteren, The GROMOS bimolecular simulation program package, J. Phys. Chem. 103 (1999) 3596–3607.
[32] Chemical Computing Group Molecular Operating Environment (MOE) Software, 2010.
[33] A. Ibezim, E. Ezechukwu, In-silico study of flavonoids from Cassia tora as potential anti- psoriatic agent, J. Appl. Pharmaceut. Sci. 9 (4) (2019) 82–87.
[34] E.A. Onoabedje, A. Ibezim, U.S. Onoabedje, U.C. Okoro, New antimicrobial leads in phenothiazine scaffold: synthesis, biological assay and virtual screening, Chemistry 2 (2017) 11954–11958.
[35] C.A. Lipinski, Drug-like properties and the causes of poor solubility and poor permeability, J. Pharmacol. Toxicol. Methods 44 (2000) 235–249.
[36] F. Ntie-Kang, N.J. Nwodo, A. Ibezim, C.V. Simoben, B. Karaman, V.F. Ngwa, W. Sippl, M.U. Adikwu, M.L. Mbaze, Molecular modeling of potential anticancer agents from African medicinal plants, J. Chem. Inf. Model. 54 (2014) 2433–2450.